Available online at www.sciencedirect.com
SCIENCE DIRECT®
Carbohydrate Research 339 (2004) 1427–1437
Carbohydrate RESEARCH

Inclusion complexes of V-amylose with undecanoic acid and dodecanol at atomic resolution: X-ray structures with cycloamylose containing 26 D-glucoses (cyclohexaicosaose) as host

Olaf Nimz,[a,†] Katrin Gessler,[a,‡] Isabel Usón,[b] George M. Sheldrick[b] and Wolfram Saenger[a,*]

[a]*Institut für Chemie/Kristallographie, Freie Universität Berlin, Takustrasse 6, D-14195 Berlin, Germany*
[b]*Institut für Anorganische Chemie, Universität Göttingen, Tammannstrasse 4, D-37077 Göttingen, Germany*

Received 25 September 2003; revised 17 February 2004; accepted 26 February 2004

Abstract—Crystal structures are reported of cycloamylose containing 26 D-glucose residues (CA26, cyclohexaicosaose, $C_{156}H_{260}O_{130}$) in complexes with undecanoic acid ($CA26{\cdot}2C_{10}H_{21}COOH{\cdot}34.95H_2O$, orthorhombic $P2_12_12_1$, one CA26 and two bound undecanoic acids F1 and F2 in the asymmetric unit, resolution 0.95 Å) and with dodecanol ($(CA26)_{0.5}{\cdot}C_{12}H_{25}OH{\cdot}32.0H_2O$, monoclinic $C2$, half a CA26 binding one dodecanol, A, in the asymmetric unit, resolution 1.0 Å). The macrocycle of CA26 is folded like the figure '8' into two 10 D-glucoses long left-handed V-amylose helices forming ~5 Å wide V-channels that are occupied by undecanoic acid (F1, F2) or dodecanol (A) as guest molecules. The functional head groups of the guests near the O(6) ends of the V-channels are hydrogen bonded with D-glucose $O(6)_n$–H; the aliphatic termini beyond C(9) protrude from the O(2), O(3) ends. Parts of the aliphatic chains enclosed in the V-channels are all-*trans* except for one torsion angle each (~130°) in undecanoic acid molecules F1 and F2. There are several (guest)C–H···O hydrogen bonds to O(4) and O(6) of CA26 in both complexes, and H···H van der Waals interactions with D-glucose C(3)–H and C(5)–H dominate. C(5)–H determine the position of the aliphatic chains of undecanoic acid F1 and of dodecanol A in contrast to F2 where both C(3)–H and C(5)–H contribute equally, probably because the V-channel is narrower than in F1 and in dodecanol. Complexes of polymeric V-amylose with fatty acids and alcohols studied by X-ray fiber diffraction could not provide the here described high resolution.

Keywords: Cyclohexaicosaose; Cycloamylose; V-Amylose; Hydrophobic channel; Fatty acid; Aliphatic alcohol; Inclusion complex

1. Introduction

Inclusion complexes between lipids and amylose are formed naturally in seeds.[1,2] They are valuable in food processing because fatty acids and their monoglyceride esters reduce stickiness of starch, improve freeze-thaw stability and have an anti-staling effect in bread and biscuits due to reduced crystallization (retrogradation) of the amylopectin fraction in starch.[3,4] If amylose is complexed with fatty acids containing 10–18 carbon atoms, X-ray diffraction in aqueous solution at temperatures of ~70 °C indicates formation of a helical structure with seven D-glucoses per turn that transforms by annealing at 90 °C to a left-handed helix with six residues per turn (6_5 symmetry) and a ~5 Å wide central channel.[5] The latter is the most frequently observed and thermodynamically stable form called V-amylose.[6]

V-Amylose is obtained from amylose by formation of inclusion complexes with small guest molecules like

* Corresponding author. Tel.: +30-83853412; fax: +30-83856702; e-mail: saenger@chemie.fu-berlin.de
† Present address: Organon Laboratories Ltd, ML1 5SH Newhouse, Scotland.
‡ Present address: Xerox GmbH, Vor dem Lauch 15, D-70567 Stuttgart, Germany.

0008-6215/$ - see front matter © 2004 Elsevier Ltd. All rights reserved.
doi:10.1016/j.carres.2004.02.030

iodine, alcohols, Me_2SO,[6,7] that are accommodated in the central channel of the V-helix, and complexes with alcohols and fatty acids (with 8–16 C-atoms) even crystallize.[8] Since the crystals are not suitable for X-ray diffraction studies due to disorder, they have been studied by X-ray fiber diffraction, spectroscopic, and calorimetric methods.[6–11] The structures of guest molecules and host–guest interactions remained, however, undetermined due to the limited resolution of X-ray fiber diffraction. They were investigated by computer-aided modeling for the complex between V-amylose and dodecanoic acid using the X-ray fiber structure of V-amylose and dodecanoic acid with ideal all-*trans* geometry.[12]

The geometry of V-amylose has been determined at atomic resolution (0.99 Å) by X-ray analysis of a cycloamylose (CA) with 26 D-glucoses in the macrocycle, CA26 hydrate, $(CA26)_2{\cdot}76.75H_2O$.[13] The CA26 macrocycle is folded like the figure '8' into a compact structure with pseudo-twofold C_2 symmetry relating two segments with 13 D-glucoses each. They are twisted into 10 D-glucoses long V-amylose left-handed single helices in antiparallel orientation that contain six D-glucoses per turn of 8.1 Å pitch height, the central channels being occupied by disordered water molecules. Since these features are characteristic of V-amylose,[6,7] CA26 is an ideal model for this polymorph of amylose.

Here we describe X-ray crystal structures of CA26 inclusion complexes with undecanoic acid and dodecanol as guests. The guest molecules are included in the V-amylose channels and provide information on guest conformation and host–guest interactions.

2. Results

2.1. Nomenclature, C–H hydrogen atoms and accuracy

Atoms of CA26 are denoted as, for example, $C(5)_{16}$ for atom C(5) in D-glucose G(16). Atoms of the two undecanoic acids F1, F2 (F for fatty acid) and dodecanol A (A for alcohol) are denoted as, for example, $C(5F_1)$, and C(5A), respectively, for atom C(5). C–H hydrogen atoms of CA26 and guest molecules were put into calculated positions[14] at C–H distances of 0.97 Å, see Section 5. Interatomic distances obtained from the least squares correlation matrices are precise at about 0.01–0.05 Å and given with only two decimal digits. The average precisions in distances are: for O(2)···O(3′), 0.01 Å; for O···O_W, 0.02 Å; for H···H in C–H···H–C and H···O in C–H···O, 0.05 Å; for torsion angles, 1.5°.

2.2. Structure of CA26

The two complexes of CA26 (Fig. 1a and b) crystallized as CA26·(undecanoic acid)$_2{\cdot}34.95H_2O$, orthorhombic $P2_12_12_1$ with one CA26 in the asymmetric unit (**CA26·F**) and $(CA26)_{0.5}{\cdot}$dodecanol$\cdot 32.0H_2O$, monoclinic $C2$, with one-half CA26 in the asymmetric unit, the other half being related by the inherent twofold rotation symmetry (C_2) (**CA26·A**) (Table 1).

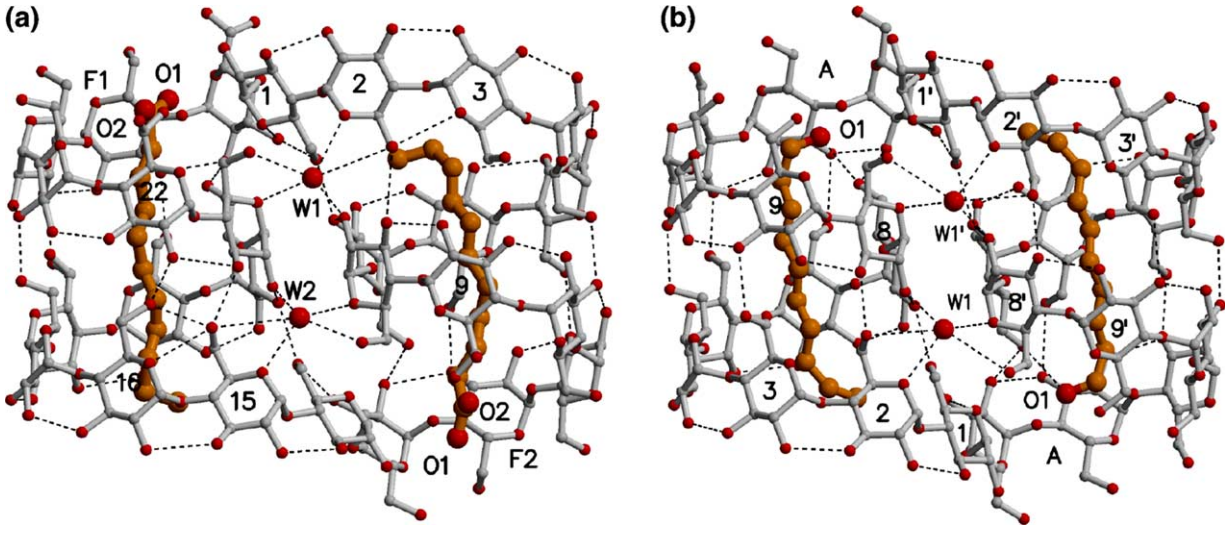

Figure 1. Views of the complexes formed (a) between CA26 and undecanoic acid molecules F1 and F2 (**CA26·F**) and (b) between CA26 and dodecanol A (**CA26·A**), with relevant water molecules indicated. D-Glucose units numbered 1 to 26 in (a) and 1 to 13, 1′ to 13′ in (b), oxygen atoms in red, carbon atoms of CA26 gray, and of guest molecules F1, F2, and A, yellow. Dashed lines indicate O–H···O hydrogen bonds; for C–H···O bonds see Figures 3a–c and 5a–c. The pseudo-symmetry axis relating the two halves of CA26, segments C1 to C13 and C14 to C26 is normal to the paper plane and located between water molecules W1, W2 in (a) and W1, W1′ in (b); water molecules W3 and W4 not shown as they are located behind and obscured by W1, W2 and W1, W1′, respectively. Drawn with Molscript and Raster3d.[31,32]

Table 1. Crystallographic data and refinement

	CA26 undecanoic acid complex	CA26 dodecanol complex
Chemical formula	$(C_{156}H_{260}O_{130})\cdot(C_{11}H_{22}O_2)_2\cdot 34.95H_2O$	$(C_{156}H_{260}O_{130})_{0.5}\cdot(C_{12}H_{25}O)\cdot 32.0H_2O$
Formula weight	5217.88	2869.66
Space group	Orthorhombic $P2_12_12_1$	Monoclinic $C2$
Unit cell constants [Å]	$a = 20.83(2)$	$a = 49.98(3)$
	$b = 27.22(2)$	$b = 13.84(1)$
	$c = 46.67(5)$	$c = 21.46(1)$
	$\alpha = \beta = \gamma = 90°$	$\alpha = \gamma = 90°$; $\beta = 114.46(3)°$
Volume [Å^3]	26,459	13,516
Calculated density [g/cm^3]	1.12	1.09
Wavelength [Å]	0.82	0.71073
Resolution range [Å]	20–0.95	22.7–1.0
Temperature [°C]	4	4
Measured reflections	191,720	51,197
Unique reflections		
All data	23,845	7442
$\geqslant 4\sigma(F_{obs})$	15,353	6897
Completeness [%]	98	100
R_{sym} [%]	5.1	5.4
Reflections used for R_{free}	1263	374
$\geqslant 4\sigma(F_{obs})$	814	273
Number of variables	2945	1563
Final R-factor		
All data	0.138	0.099
With $\geqslant 4\sigma(F_{obs})$	0.095	0.074
R_{free}		
All data	0.164	0.120
With $\geqslant 4\sigma(F_{obs})$	0.119	0.088
Data/parameter		
$\geqslant 4\sigma(F_{obs})$	8.1 (5.2)	4.6 (4.3)
GooF	1.522	0.978
$\Delta(\rho)$max, $\Delta(\rho)$min [e/Å^3]	0.52, −0.48	0.52, −0.32

The structures of CA26 in **CA26·F** and **CA26·A** are comparable to those in CA26*o* ($CA26\cdot 32.59H_2O$, orthorhombic),[15] CA26*ta* and CA26*tb* in ($(CA26)_2\cdot 76.75H_2O$, triclinic, molecules *a* and *b*)[13] and $CA26\cdot 6NH_3I_3\cdot 2NH_4I\cdot 91.5H_2O$, $(CA26)_{0.5}\cdot Ba_{0.5}I_3\cdot (PEG400)_{0.5}\cdot glycol\cdot 23.75H_2O$.[16] The root mean square (rms) deviations for superposition of CA26 (O(6)–H groups and H-atoms omitted) in these crystal structures are in the range 0.31–0.80 Å, suggesting that the conformations of the CA26 molecules are only little influenced by crystal packing forces or guest molecules. CA26 is divided into two halves, D-glucose residues G(1) to G(13) and G(14) to G(26) that are related to each other by a pseudo-twofold (pseudo-C_2) or by a crystallographic twofold rotation axis (C_2), respectively. The pseudo-C_2 or C_2 symmetry is obvious from the D-glucose numbering (G(*n*)) in Figure 1a and b. In Figure 1a, for $n < 14$, G(*n*) is related to G($n + 13$) and for $n > 13$, G(*n*) is related to G($n - 13$); in Figure 1b, G(*n*) is identical to G(n') as they are related by the crystallographic C_2 symmetry.

The molecular halves in all CA26 are cross-linked by four conserved water molecules W1 to W4 (except for CA26*o*[15] where W3 is replaced by $O(6)_{22}$–H) that are related by the pseudo-C_2 symmetry, W1 corresponding to W2 and W3 to W4; in Figure 1a only W1 and W2 are shown (caption of Fig. 1). These water confer stability to the folding of CA26 by hydrogen bonding ($O\cdots O_W$ at 2.81–3.46 Å) in bidentate mode to O(5)/O(6) or to O(2)/O(3) (Fig. 1a).

Each of the halves of CA26 in **CA26·F** and **CA26·A** features a V-helix defined by 10 D-glucoses G(3) to G(12) and G(16) to G(25). Torsion angles χ(O(5)–C(5)–C(6)–O(6)) are predominantly (−)-*gauche*, that is, the O(6) groups point away from the central channel and stabilize the 6 D-glucoses long V-helical turns by hydrogen bonds $O(6)_n\cdots O(2)_{n+6}$/$O(3)_{n+6}$ (2.71–3.38 Å). Their central cavities with van der Waals diameter of 5–5.5 Å[13] are occupied by undecanoic acid or dodecanol molecules. Because D-glucoses in segments G(1) to G(13) and G(14) to G(26) are oriented the same way (*syn*), hydrogen bonds $O(3)_n\cdots O(2)_{n+1}$ between adjacent D-glucose residues along the chain (2.72–3.18 Å) form a continuous band. By contrast, D-glucoses in the pairs G(13)–G(14) and G(26)–G(1) connecting the two halves of CA26 are oriented *anti* in a conformation that was termed band-flip[13,15–19] because the continuous band is interrupted here.

The band-flips in **CA26·F** and **CA26·A** are stabilized by three-center (bifurcated) intramolecular, interglucose hydrogen bonds[13,15–19] formed between O(3)–H of G(26)

and G(13) as donors and O(5)/O(6) of G(1) and G(14) as acceptors (2.80–3.00 Å). In addition, hydrogen bonds $O(6)_1$–H···$O(2)_7/O(3)_7$; $O(6)_{14}$–H···$O(2)_{20}/O(3)_{20}$ and water mediated interactions $O(2)_7$···W3···$O(2)_{26}/O(3)_{26}$; $O(2)_{20}$···W4···$O(2)_{13}/O(3)_{13}$ (2.65–3.47 Å) are associated with the band-flips. Torsion angles χ of D-glucoses G(1), G(7) and the pseudo-C_2 related G(14), G(20) are conserved in (+)-*gauche* and rotated toward the channel of the V-helix because they are associated with the two band-flips.[13,19] This geometry is again conserved in all CA26 structures studied thus far, suggesting that it is an intrinsic feature of the characteristic folding pattern of CA26.

2.3. Undecanoic acid molecules are enclosed in the V-channels of CA26·F

The $C(10F_{1,2})$–$C(11F_{1,2})$ termini of F1 and F2 protrude from the O(2), O(3) sides of the V-channels and the carboxyl groups are located at the O(6) sides (Fig. 1a). They are protonated, –COOH, according to strong Raman bands of the crystals at 1610 and 1649 cm^{-1} (not shown). The two bands must be associated with different environments of the –COOH groups since pure undecanoic acid exhibits a single band at 1657 cm^{-1}.

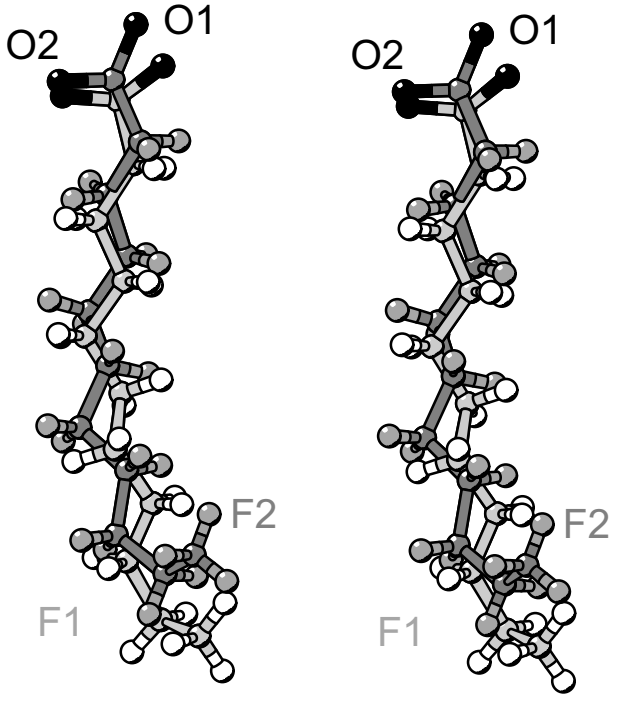

Figure 2. Stereo view of F1 and F2 (light and dark gray, respectively) obtained by superimposing the V-helical segments G(1)–G(13) and G(14)–G(26) of **CA26·F**. The large deviations at the CH_2–CH_3 terminus are due to C–H···O hydrogen bonds of $C(11F_2)H_3$ with $O(2)_7$ and $O(3)_7$ that are not formed with F1 (see Fig. 3a and b). Drawn with Molscript.[31]

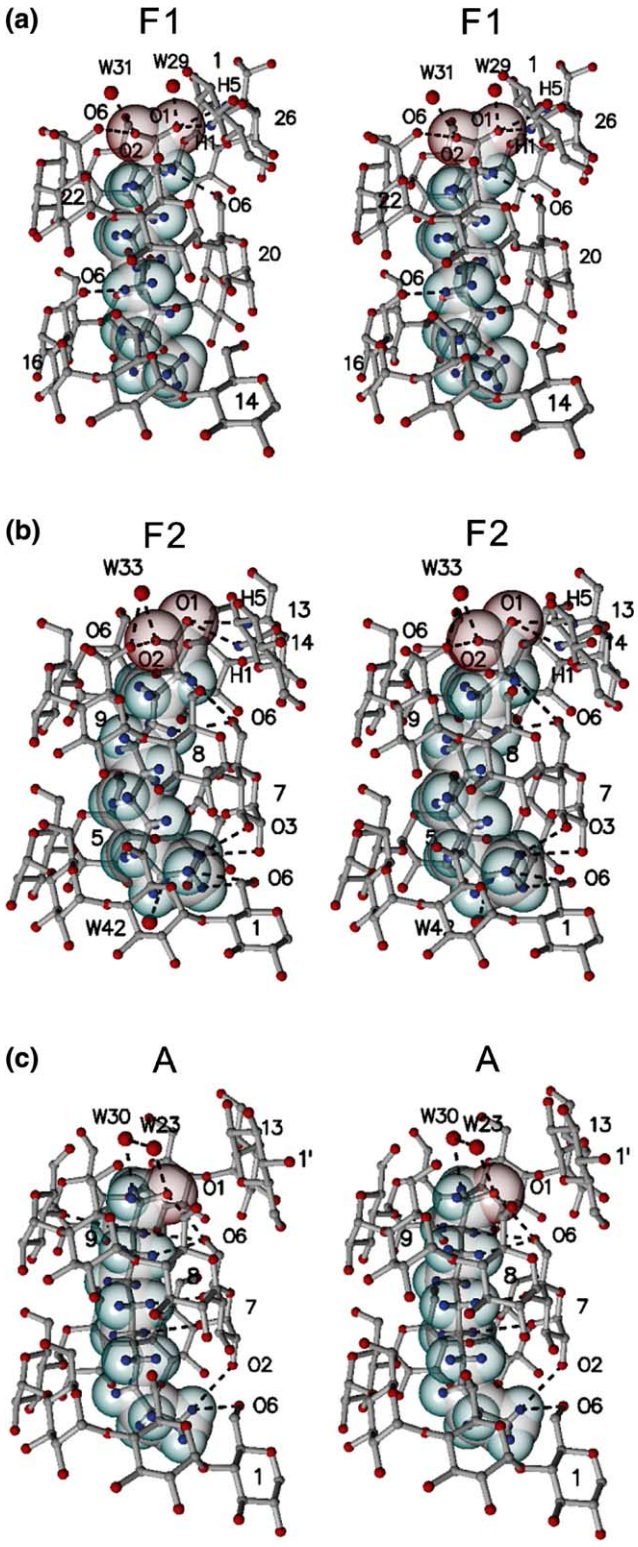

Figure 3. Stereo views of complexes formed between CA26 and undecanoic acids F1 (a), F2 (b) and dodecanol A (c). Van der Waals radii of F1, F2, and A drawn as spheres. Oxygen red, hydrogen blue, relevant atoms labeled, hydrogen bonds O–H···O and C–H···O <3.4 Å indicated by dashed lines. View directions are different to Figure 1 to show hydrogen bonding of carbohydrate O–H and C–H groups. Drawn with Molscript and Raster3d.[31,32]

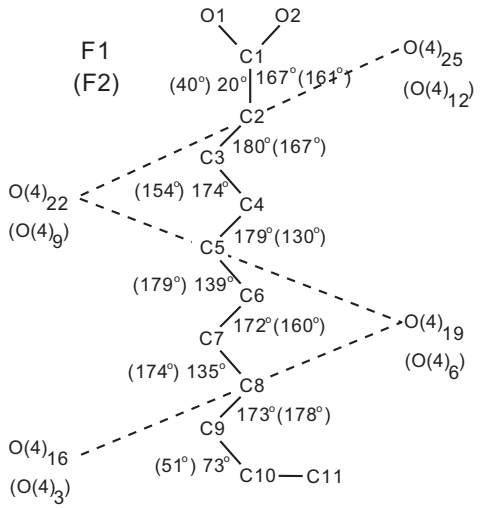

Figure 4. Torsion angles of undecanoic acid molecules F1 and F2 (with numbers for F2 in parentheses) are written near the central bond. The orientation with respect to CA26 is indicated by the dashed zigzag line that connects O(4) atoms of CA26, that is, the planes defined by $O(4)_{16,\,19,\,22,\,25}$ and by $O(4)_{3,\,6,\,9,\,12}$ coincide with the planes defined by C(2) to C(8) of F1 and F2, respectively.

Superposition of the pseudo-C_2 related halves of **CA26·F** (excluding $C(10F_{1,2})$–$C(11F_{1,2})$ as they adopt different positions described below) matches F1 and F2 positionally with rms deviation 0.58 Å (Fig. 2). The central parts of the aliphatic chains match poorly as they are severely distorted from an ideal all-*trans* conformation.

The carboxyl groups of F1 and F2 are differently hydrated (Fig. 3a and b). Oxygen atoms $O(2F_1)$, $O(2F_2)$ form hydrogen bonds with (+)-*gauche* oriented $O(6)_{22}$ and $O(6)_9$ (both disordered (+) and (−)-*gauche*) while $O(1F_{1,2})$ accept C–H···O hydrogen bonds, $O(1F_1)$ being chelated by $C(1)_1$–H, $C(5)_{26}$–H and $C(5)_{25}$–H (the latter is hidden in Fig. 3a) and $O(1F_2)$ by $C(1)_{14}$–H and $C(5)_{13}$–H (2.35–3.04 Å) (Fig. 3b). These C–H···O interactions are due to the band-flips as G(26) and G(13) provide C(5)–H as hydrogen bond donor but D-glucoses G(1) and G(14) are flipped by ∼180° in *anti*-conformation and consequently donate with C(1)–H.

The $C(11F_{1,2})H_3$ termini adopt (+)-*gauche* conformations and are in contact with the inner surface at the O(2), O(3) ends of the V-channels (Figs. 3a, b and 4). F1 forms only one short H···H contact at 2.39 Å with CA26, $C(10F_1)$–H···H–$C(3)_{18}$ (not shown in Fig. 3a, see Table 2), whereas F2 donates four C–H···O hydrogen bonds (Fig. 3b), two each with $O(6)_1$ and $O(2)_7$/$O(3)_7$ at 3.06–3.27 Å.

The parts of the aliphatic chains that are fully enclosed in the V-channels ($C(2F_{1,2})$ to $C(9F_{1,2})$) are

Table 2. Distances H···H <2.80 Å and H···O <3.40 Å between F1, F2, A, and CA26[a]

H-atoms F1	H-atoms CA26	H···H	H-atoms F2	H-atoms CA26	H···H	H-atoms A	H-atoms CA26	H···H
$C(10F_1)$–HB	$C(3)_{18}$–H	2.39	$C(9F_2)$–HB	$C(5)_3$–H	2.56	C(7A)–HA	$C(6)_2$–HB	2.76
$C(9F_1)$–HA	$C(5)_{17}$–H	2.44	$C(9F_2)$–HB	$C(6)_2$–HB	2.71	C(7A)–HA	$C(5)_3$–H	2.72
$C(9F_1)$–HB	$C(6)_{15}$–HB	2.22	$C(9F_2)$–HA	$C(5)_4$–H	2.71	C(7A)–HB	$C(3)_7$–H	2.47
$C(9F_1)$–HB	$C(5)_{16}$–H	2.76	$C(8F_2)$–HB	$C(3)_7$–H	2.69	C(6A)–HA	$C(5)_4$–H	2.76
$C(8F_1)$–HA	$C(5)_{18}$–H	2.78	$C(7F_2)$–HB	$C(5)_4$–H	2.61	C(6A)–HA	$C(6)_4$–HB	2.77
$C(6F_1)$–HA	$C(5)_{18}$–H	2.68	$C(7F_2)$–HB	$C(6)_4$–HA	2.50	C(6A)–HA	$C(5)_5$–H	2.57
$C(6F_1)$–HB	$C(5)_{20}$–H	2.60	$C(7F_2)$–HB	$C(6)_4$–HB	2.50	C(6A)–HB	$C(5)_6$–H	2.77
$C(6F_1)$–HB	$C(5)_{19}$–H	2.78	$C(7F_2)$–HA	$C(3)_8$–H	2.80	C(5A)–HB	$C(5)_7$–H	2.73
$C(5F_1)$–HA	$C(3)_{23}$–H	2.74	$C(6F_2)$–HB	$C(5)_6$–H	2.80	C(5A)–HB	$C(3)_8$–H	2.63
$C(4F_1)$–HA	$C(5)_{20}$–H	2.51	$C(6F_2)$–HA	$C(3)_8$–H	2.61	C(4A)–HA	$C(6)_5$–HB	2.68
$C(4F_1)$–HA	$C(5)_{21}$–H	2.69	$C(5F_2)$–HA	$C(3)_9$–H	2.62	C(4A)–HA	$C(5)_6$–H	2.79
$C(4F_1)$–HA	$C(6)_{20}$–HA	2.74	$C(5F_2)$–HB	$C(3)_{10}$–H	2.67	C(3A)–HA	$C(5)_8$–H	2.38
$C(3F_1)$–HA	$C(5)_{22}$–H	2.52	$C(4F_2)$–HB	$C(3)_{11}$–H	2.60	C(3A)–HB	$C(5)_9$–H	2.52
$C(2F_1)$–HB	$C(3)_{25}$–H	2.69	$C(3F_2)$–HA	$C(5)_9$–H	2.54	C(2A)–HB	$C(3)_{11}$–H	2.59
			$C(3F_2)$–HB	$C(5)_{11}$–H	2.64	C(1A)–HA	$C(5)_{11}$–H	2.72
			$C(2F_2)$–HA	$C(3)_{12}$–H	2.58	C(1A)–HB	$C(5)_9$–H	2.73
			$C(2F_2)$–HA	$C(5)_{12}$–H	2.71			
	O-atoms CA26	H···O		O-atoms CA26	H···O		O-atoms CA26	H···O
$C(9F_1)$–HA	$O(4)_{16}$	3.38	$C(11F_2)$–HB	$O(6)_1$	3.27	C(10A)–HB	$O(6)_1$	2.86
$C(8F_1)$–HA	$O(4)_{18}$	3.09	$C(11F_2)$–HA	$O(6)_1$	3.06	C(10A)–HB	$O(2)_7$	3.11
$C(7F_1)$–HA	$O(6)_{16}$	2.94	$C(11F_2)$–HC	$O(2)_7$	3.15	C(6A)–HB	$O(4)_6$	3.20
$C(7F_1)$–HB	$O(4)_{20}$	3.37	$C(11F_2)$–HC	$O(3)_7$	3.10	C(5A)–HB	$O(4)_7$	2.83
$C(5F_1)$–HB	$O(4)_{21}$	3.18	$C(6F_2)$–HA	$O(4)_7$	3.19	C(3A)–HA	$O(6)_7$	3.15
$C(4F_1)$–HA	$O(6)_{20}$	3.06	$C(5F_2)$–HA	$O(4)_9$	3.14	C(2A)–HA	$O(6)_7$	3.19
$C(3F_1)$–HB	$O(4)_{23}$	3.05	$C(4F_2)$–HA	$O(6)_7$	2.98	C(2A)–HB	$O(4)_{10}$	2.98
$C(2F_1)$–HA	$O(6)_{20}$	2.77	$C(3F_2)$–HB	$O(4)_{10}$	3.26			
$C(2F_1)$–HB	$O(4)_{24}$	3.01	$C(2F_2)$–HA	$O(6)_7$	3.08			
$C(2F_1)$–HB	$O(6)_{20}$	3.32	$C(2F_2)$–HB	$O(6)_7$	3.02			
			$C(2F_2)$–HA	$O(4)_{12}$	3.25			

[a] A, B, and C after H indicate different H-atoms at CH_2 and CH_3 groups.

all-*trans* (154–180°) with one exception each in F1 and F2, see below. The plane defined by carbon atoms $C(2F_1)$ to $C(8F_1)$ of F1 coincides with the plane defined by $O(4)_{16}$–$O(4)_{19}$–$O(4)_{22}$–$O(4)_{25}$ of the CA26 host (Figs. 4 and 5), and the plane of F2 coincides with the pseudo-C_2 symmetry related plane $O(4)_3$–$O(4)_6$–$O(4)_9$–$O(4)_{12}$.

Short H···H and C–H···O interactions with cut-off distances <2.80 Å for H···H and <3.40 Å for H···O, respectively, are formed in the V-channels between CA26 and F1, F2 (Table 2; Fig. 5a and b). These interactions do not follow the pseudo-C_2 symmetry, see for instance differences in short H···H and H···O contacts formed by $C(7F_1)$–H and $C(7F_2)$–H and by other $C(F_{1,2})$–H groups (Table 2).

Within the V-channels, 10 and 9 short C–H···O interactions involve aliphatic C–H groups and D-glucose oxygen atoms O(4)/O(6) in the ratios 6/4 for F1 and 4/5 for F2, respectively (Table 2) with all O(6) in (+)-*gauche*. In F1, three C–H donors (two from $C(2F_1)$–H and one from $C(4F_1)$–H) chelate $O(6)_{20}$ (that is engaged in the band-flip). Similarly, the pseudo-C_2 related $O(6)_7$ is chelated by $C(4F_2)$–H and two $C(2F_2)$–H. One of the four (guest)C–H···O(6) hydrogen bonds in F1 is formed with $O(6)_{16}$ that is in the channel with unique (+)-*gauche* orientation, $C(7F_1)$–H···$O(6)_{16}$ at 2.94 Å (Table 2 and Fig. 3a). This hydrogen bond distorts the all-*trans* form of the F_1 aliphatic tail by out-of-plane bending of $C(7F_1)$, accompanied with torsion angles at 139° and 135° (Fig. 4). The geometry of F2 is different at $C(7F_2)$ as the pseudo-C_2 related $O(6)_3$ is in common (−)-*gauche* and cannot form this interaction. Six (guest)C–H···O(4) hydrogen bonds in F1 (to $O(4)_{16,18,20,21,23,24}$) and four in F2 (to $O(4)_{7,9,10,12}$), range 3.01–3.38 Å (Table 2). depend only on the conformations of the aliphatic chains and of the V-helices and not on end effects. They may occur generally in complexes between aliphatic chains and polymeric V-amylose.

H···H contacts between guests and C(3)–H/C(5)–H/C(6)–H of CA26 are distributed in ratios 3/9/2 for F1 (2.22–2.78 Å) and 7/7/3 for F2 (2.50–2.71 Å). H···H distances to F1 are between 0.1 and 0.28 Å shorter than those to F2, suggesting that these host–guest interactions are tighter in F1 than in F2. For F1, the preferred 9 interactions with C(5)–H agree with the modeled complex between polymeric V-amylose and all-*trans* dodecanoic acid where the distances of C(5)–H to the hydrogen atoms of the aliphatic chain were found shortest (2.33–2.38 Å) and decisive for the orientation of the aliphatic chain in the V-channel.[12] The preference for C(5)–H is associated with the conical shape of the V-helical turns in which C(6) (and C(5)–H) are closer to the helical axis than O(2), O(3) (and C(3)–H) (see Fig. 5a), thereby favoring C(5)–H for H···H interactions with the guest molecule.

By contrast, H···H contacts between F2 and CA26 indicate that C(3)–H and C(5)–H contribute equally (7 each) (see Table 2 and Fig. 5b). $C(4F_2)$–H and $C(5F_2)$–H in this segment of F2 are part of torsion angles at 154° and at 130° (Fig. 4), suggesting that this distortion of the all-*trans* conformation of the aliphatic chain is associated with the abundance in short H···H interactions involving C(3)–H of F2. Since C(3)–H groups allow for more space than C(5)–H groups, this even permits the aliphatic chain of F2 to be tilted with respect to the axis of the V-channel, compare Figure 5a (F1 chain is vertical to the paper plane) with Figure 5b (F2 chain is tilted).

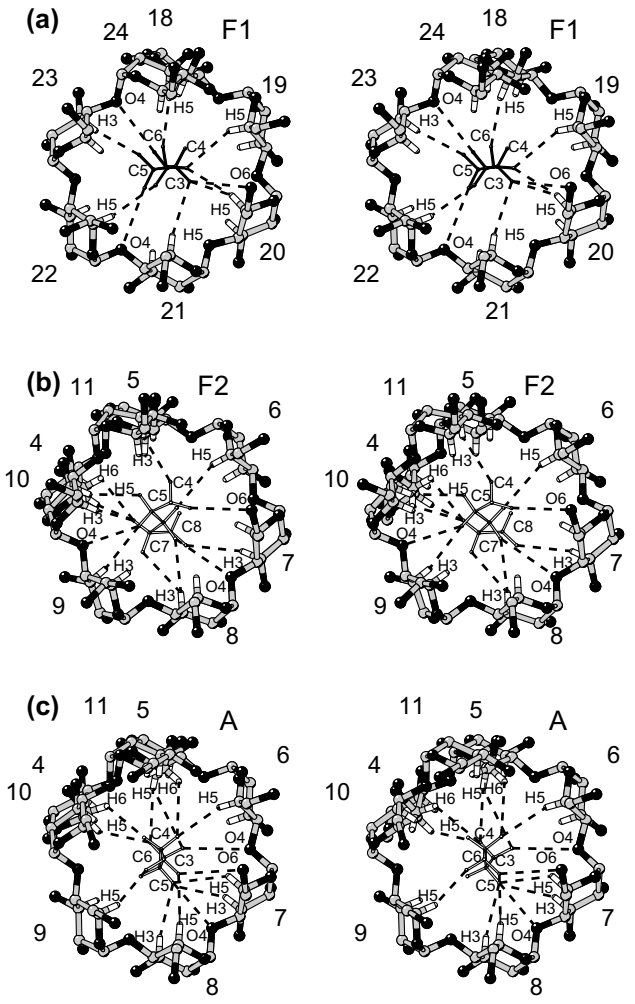

Figure 5. Stereo views (drawn at the same scale and orientation) of sections of the complexes formed between CA26 and undecanoic acids F1 (a, $C(3F_1)$ to $C(6F_1)$), F2 (b, $C(4/F_2)$ to $C(8F_2)$) and dodecanol A (c, C(3A) to C(6A)) showing host–guest interactions in the center of the V-channels. Short H···H and C–H···O and interactions <2.80 and <3.40 Å, respectively, are indicated by broken lines, oxygen atoms black, C(3)–H and C(5)–H hydrogen atoms white. View direction is along the axis of the V-channel. Note that in (a) CH_2 groups $C(3F_1)$, $C(4F_1)$, $C(5F_1)$ are staggered but $C(6F_1)$ is eclipsed due to torsion angle $C(4F_1)$–$C(5F_1)$–$C(6F_1)$–$C(7F_1)$, 139°, and there are more H···H contacts to C(5)–H of CA26 than in (b) where contacts to C(3)–H dominate, permitting the aliphatic chain to be even tilted against the axis of the V-helix.

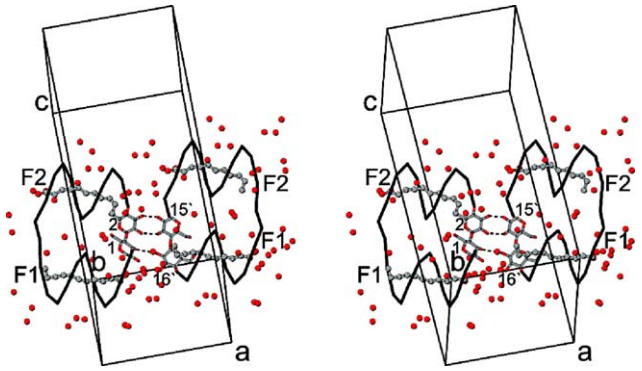

Figure 6. Stereo view showing hydrogen bonding interactions between CA26 molecules in the crystal lattice of **CA26·F**. D-Glucoses forming O(2)···O(3′) hydrogen bonds (dotted lines) are shown in ball-and-stick presentation, the backbone of CA26 is indicated by virtual bonds connecting O(4) atoms, water, and carboxyl oxygen atoms are shown as red spheres. O···O distances are: $O(3)_2\cdots O(2')_{15}$ 2.73 Å; $O(2)_2\cdots O(3')_{15}$ 2.68 Å; $O(3)_1\cdots O(2')_{16}$ 3.35 Å. Drawn with Molscript.[31]

The crystal packing of **CA26·F** (Fig. 6) is stabilized by hydrogen bonds between G(1), G(2) and G(15′), G(16′) of *a*-translation related CA26 [indicated by (′)]; distances in caption of Figure 6. The V-channels of adjacent CA26 are oriented nearly parallel but not collinear. The $C(10F_{1,2})$–$C(11F_{1,2})$ termini protrude from the channels and are separated from the carboxyl groups of *a*-translation related molecules by about 9 Å, the voids being filled by water.

2.4. Dodecanol molecules are enclosed in the V-channels of CA26·A

The dodecanol hydroxyl group is near the O(6) side of the V-channel (Figs. 1b and 3c), and the C(11A)–C(12A) group is positionally disordered and not seen in the electron density. The torsion angles at both ends of dodecanol are (+)-*gauche*, 73° at the head and 70° at the tail, the others in the range 142–179° (Fig. 7). The zigzag plane defined by C(2A) to C(8A) coincides with the plane defined by $H(5)_2$–$H(5)_5$–$H(5)_8$–$H(5)_{11}$ of CA26 (Fig. 7) and is nearly normal to the plane defined by undecanoic acids F1 and F2 (see Fig. 5a and b).

Dodecanol is inserted deeper in the V-channel than undecanoic acid, compare Figure 3a and b with Figure 3c. The alcohol hydroxyl forms one hydrogen bond with the host molecule, $O(1A)\cdots O(6)_7$ 3.16 Å with $O(6)_7$ in (+)-*gauche* orientation and to W23 ($O(1A)\cdots O_{W23}$ 2.81 Å) and there are no (host)C–H···O(1A) interactions, contrasting **CA26·F**. W23 and W30 hydrogen bond to the five O(6) hydroxyl groups (all in (+)-*gauche* orientation) of D-glucoses G(9) to G(13) (Figs. 3c and 8). Such pattern has not previously been observed with any of the CA26 structures where these O(6) hydroxyl groups are (−)-*gauche*[13,15] and in **CA26·F** only O(6) of

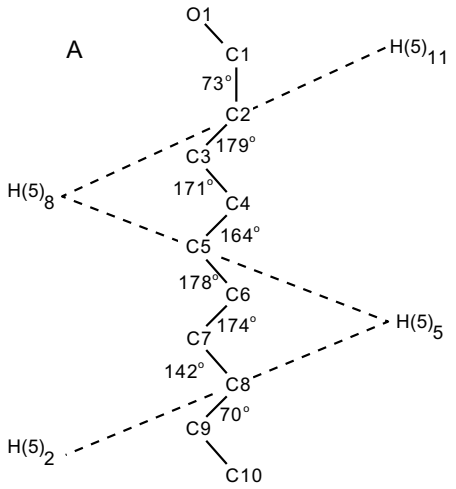

Figure 7. Torsion angles of the dodecanol in **CA26·A**. The plane formed by CA26 atoms $H(5)_{2,5,8,11}$ coincides with the plane defined by dodecanol atoms C(2A) to C(8A). Atoms C(11A) and C(12A) not drawn as they could not be identified in the electron density map.

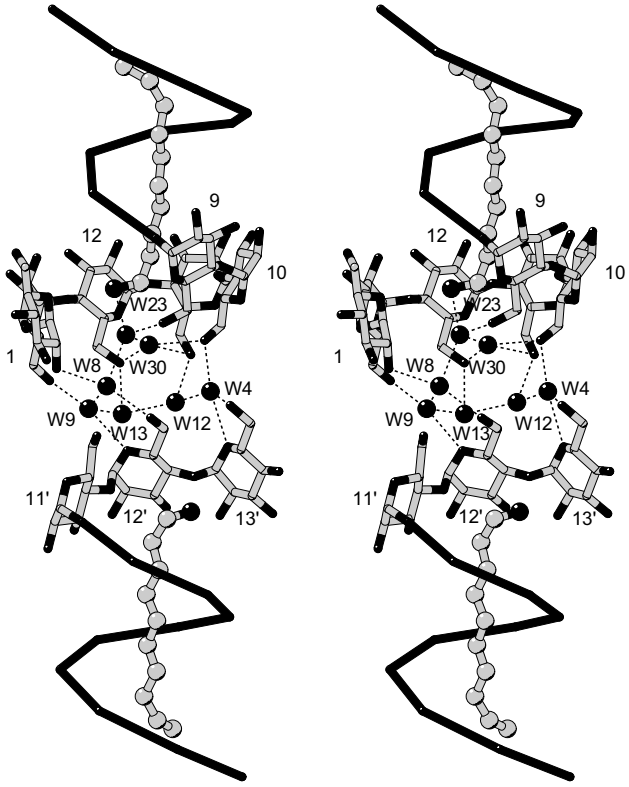

Figure 8. In the crystal structure of **CA26·A**, an intermolecular interaction is mediated by a chain of five water molecules that are also hydrogen bonded through W23 to the hydroxyl group of dodecanol. The two CA26 molecules with unprimed and primed (′) atoms [(top) and (bottom)] are related by C_2 symmetry, the twofold rotation axis being nearly horizontal and passing between the two CA26 molecules. Note (+)-*gauche* orientation of O(6) hydroxyl groups of G(10) to G(13). Drawn with Molscript.[31]

G(13) is (+)-*gauche*. The C-terminus of A forms a bifurcated C–H···O hydrogen bond that connects G(1)

Table 3. (a) H···H distances (Å) defined by $C(5)_n$–H···H–$C(3)_{n+3}$ across the V-channels in **CA26·F** accommodating undecanoic acids F1, F2 and in **CA26·A** accommodating dodecanol A; (b) hydrogen bonds $O(3)_n\cdots O(2)_{n+1}$ (Å) between adjacent D-glucoses in **CA26·F** and **CA26·A**; (c) average distances of H···H and $O(3)_n\cdots O(2)_{n+1}$ of values given in Panels a and b. Root mean square (rms) deviations calculated between helical segments complexing F1, F2, A (defined by G(4)–G(10) and G(17)–G(23), omitting O(6))

	F1			F2			A	
H-atoms CA26F1	H-atoms CA26F1	H···H	H-atoms CA26F2	H-atoms CA26F2	H···H	H-atoms CA26A	H-atoms CA26A	H···H
Panel a								
$C(5)_{15}$–H	$C(3)_{18}$–H	7.99	$C(5)_2$–H	$C(3)_5$–H	8.63	$C(5)_2$–H	$C(3)_5$–H	8.35
$C(5)_{16}$–H	$C(3)_{19}$–H	7.32	$C(5)_3$–H	$C(3)_6$–H	7.29	$C(5)_3$–H	$C(3)_6$–H	7.27
$C(5)_{17}$–H	$C(3)_{20}$–H	7.29	$C(5)_4$–H	$C(3)_7$–H	7.31	$C(5)_4$–H	$C(3)_7$–H	6.83
$C(5)_{18}$–H	$C(3)_{21}$–H	7.50	$C(5)_5$–H	$C(3)_8$–H	7.06	$C(5)_5$–H	$C(3)_8$–H	7.21
$C(5)_{19}$–H	$C(3)_{22}$–H	7.96	$C(5)_6$–H	$C(3)_9$–H	7.40	$C(5)_6$–H	$C(3)_9$–H	7.47
$C(5)_{20}$–H	$C(3)_{23}$–H	7.36	$C(5)_7$–H	$C(3)_{10}$–H	7.32	$C(5)_7$–H	$C(3)_{10}$–H	7.04
$C(5)_{21}$–H	$C(3)_{24}$–H	6.94	$C(5)_8$–H	$C(3)_{11}$–H	7.14	$C(5)_8$–H	$C(3)_{11}$–H	7.20
$C(5)_{22}$–H	$C(3)_{25}$–H	7.80	$C(5)_9$–H	$C(3)_{12}$–H	7.46	$C(5)_9$–H	$C(3)_{12}$–H	7.31
$C(5)_{23}$–H	$C(3)_{26}$–H	8.46	$C(5)_{10}$–H	$C(3)_{13}$–H	8.47	$C(5)_{10}$–H	$C(3)_{13}$–H	8.17
O-atoms CA26F1	O-atoms CA26F1	O···O	O-atoms CA26F2	O-atoms CA26F2	O···O	O-atoms CA26A	O-atoms CA26A	O···O
Panel b								
$O(3)_{14}$	$O(2)_{15}$	2.79	$O(3)_1$	$O(2)_2$	2.78	$O(3)_1$	$O(2)_2$	2.97
$O(3)_{15}$	$O(2)_{16}$	3.04	$O(3)_2$	$O(2)_3$	2.81	$O(3)_2$	$O(2)_3$	2.82
$O(3)_{16}$	$O(2)_{17}$	2.82	$O(3)_3$	$O(2)_4$	2.73	$O(3)_3$	$O(2)_4$	2.73
$O(3)_{17}$	$O(2)_{18}$	2.75	$O(3)_4$	$O(2)_5$	2.83	$O(3)_4$	$O(2)_5$	2.79
$O(3)_{18}$	$O(2)_{19}$	2.97	$O(3)_5$	$O(2)_6$	3.10	$O(3)_5$	$O(2)_6$	2.78
$O(3)_{19}$	$O(2)_{20}$	2.88	$O(3)_6$	$O(2)_7$	2.81	$O(3)_6$	$O(2)_7$	2.77
$O(3)_{20}$	$O(2)_{21}$	2.73	$O(3)_7$	$O(2)_8$	2.72	$O(3)_7$	$O(2)_8$	2.75
$O(3)_{21}$	$O(2)_{22}$	3.18	$O(3)_8$	$O(2)_9$	2.74	$O(3)_8$	$O(2)_9$	2.80
$O(3)_{22}$	$O(2)_{23}$	2.83	$O(3)_9$	$O(2)_{10}$	2.81	$O(3)_9$	$O(2)_{10}$	2.76
$O(3)_{23}$	$O(2)_{24}$	2.81	$O(3)_{10}$	$O(2)_{11}$	2.78	$O(3)_{10}$	$O(2)_{11}$	2.90
$O(3)_{24}$	$O(2)_{25}$	2.92	$O(3)_{11}$	$O(2)_{12}$	2.78	$O(3)_{11}$	$O(2)_{12}$	2.87
$O(3)_{25}$	$O(2)_{26}$	2.85	$O(3)_{12}$	$O(2)_{13}$	2.97	$O(3)_{12}$	$O(2)_{13}$	2.81

	Average distances		
	$C(5)_n$–H···H–$C(3)_{n+3}$ (Å)	$O(3)_n\cdots O(2)_{n+1}$ (Å)	Rms deviations (Å)
Panel c			
F1	7.52	2.90	F1/F2 0.297
F2	7.27	2.83	F1/A 0.378
A	7.20	2.79	F2/A 0.233

and G(7) thereby bridging one V-turn, C(10A)–H···$O(6)_1$ 2.86 Å with $O(6)_1$ in (+)-*gauche* orientation and C(10A)–H···$O(2)_7$ 3.11 Å (Fig. 3c).

The aliphatic chain of A is stabilized by H···H interactions with C(3)–H/C(5)–H/C(6)–H of CA26 (2.38–2.79 Å, Table 2). The numbers of these contacts are distributed in the ratio 3/10/3 (that is comparable to F1, ratio 3/9/2) and indicate that interactions with C(5)–H determine the orientation of dodecanol in the V-channel. Additionally, five C–H···O interactions are formed to O(4)/O(6) in the ratio 3/2 with distance range 2.83–3.20 Å. (Table 2 and Fig. 3c), whereas about twice as many (10 and 9) are found in **CA26·F**.

For the V-amylose segment G(5) to G(11), the average $O(3)_n\cdots O(2)_{n+1}$ distance, 2.79 Å (Table 3b and c), is typical of γ-cyclodextrin and similar to the V-channel of F2, see above. The similarity of the V-channels enclosing

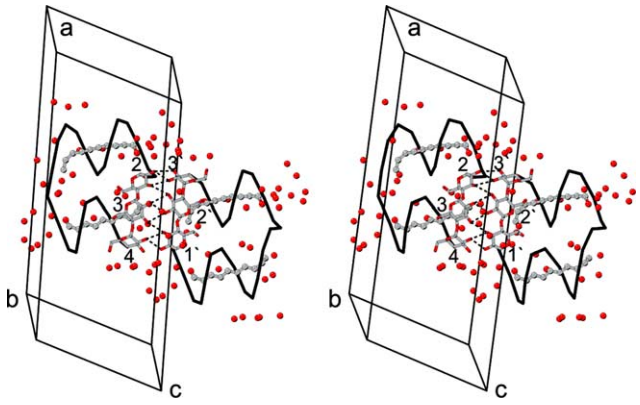

Figure 9. Crystal packing scheme of **CA26·A**, for further details see caption of Figure 6. Hydrogen bonds: $O(2)_4\cdots O(2')_1/O(3')_1$; $O(3)_3\cdots O(3')_1$; $O(2)_3/O(3)_3\cdots O(2')_2$; $O(2)_3/O(3)_2\cdots O(3')_2$; $O(3)_2/O(2)_2\cdots O(2')_3$; $O(2)_2\cdots O(3')_3$ are at 2.75–3.34 Å.

F2 and A and the dissimilarity of the V-channels enclosing F1 and A or F1 and F2 are mirrored in the respective rms deviations (Table 3c).

The all-*trans* conformation of dodecanol (torsion angles 164–179°), is better preserved than that of undecanoic acids F1 and F2 (Fig. 7). Only torsion angle C(6A)–C(7A)–C(8A)–C(9A), 142°, deviates because atom C(9A) is near the disordered C-terminus of the aliphatic chain.

The crystal packing of **CA26·A** (Fig. 9) is stabilized by direct hydrogen bonds between G(4), G(3), G(2) of one CA26 and G(1′), G(2′), G(3′) of *a*-translation related CA26 (see caption of Fig. 9). A second interaction between O(6) groups of C_2-symmetry related CA26 is mediated by the chain W8···W9···W13···W12···W4 linked through W23 with the alcohol O–H group (Fig. 8). W23 hydrogen bonds W30 that interacts with the O(6) groups of G(10), G(11), and G(12) in (+)-*gauche* orientation.

2.5. The geometry of V-amylose

A quantitative measure of the width of a V-channel can be defined by distances between hydrogen atoms $C(5)_n$–H and $C(3)_{n+3}$–H that are at about the same height in the V-channel and diametrically opposed (Table 3a). In **CA26·F**, for the seven innermost D-glucose units (G(16) to G(22)) harboring F1 and the pseudo-C_2 related (G(3) to G(9)) harboring F2, the average $C(5)_n$–H···H–$C(3)_{n+3}$ distances are 7.52 Å (range 7.29–7.96 Å) and 7.27 Å (range 7.06–7.40 Å), respectively (Table 3a and c). The average distances show that the V-channel occupied by F1 is 0.25 Å wider than that occupied by F2. In **CA26·A**, the corresponding distances for the seven innermost D-glucose units G(3) to G(9) are at 6.83–7.47 Å, average 7.20 Å, even shorter than for the F2-channel (Table 3a and c).

In addition, as shown for α-, β-, and γ-cyclodextrins with 6, 7, and 8 D-glucose units in the macrocycle, respectively, the curvature of the respective amylose segment is reflected by the average hydrogen bond lengths $O(3)_n\cdots O(2)_{n+1}$ between adjacent D-glucoses (Table 3b and c) that are 3.3 Å (α), 2.9 Å (β) and 2.8 Å (γ), each with about 0.1 Å precision.[19,20] In **CA26·F**, the average $O(3)_n\cdots O(2)_{n+1}$ distances in the V-amylose segments (G(18) to G(24)) for F1 and (G(5) to G(11)) for F2 are 2.90 Å (range 2.73–3.18 Å), and 2.83 Å (range 2.72–3.10 Å), respectively (Table 3b and c). They show that the $O(3)_n\cdots O(2)_{n+1}$ distance for the V-channel accommodating F1 (2.90 Å) is typical for β-cyclodextrin, whereas the V-channel accommodating F2 (2.82 Å) resembles γ-cyclodextrin. For the amylose segment G(5) to G(11) in **CA26·A**, the $O(3)_n\cdots O(2)_{n+1}$ distances are at 2.75–2.90 Å, average 2.79 Å (Table 3b and c), similar to the V-channel of F2, and typical of γ-cyclodextrin. The similarity of the V-channels enclosing F2 and A and the dissimilarity of the V-channels enclosing F1 and A or F1 and F2 are mirrored in the respective rms deviations of segments G(4)–G(10) and G(17)–G(23) (omitting O(6)) (Table 3c).

The $C(5)_n$–H···H–$C(3)_{n+3}$ distances provide a good estimate of the diameter of the V-channel. If the van der Waals radius of hydrogen, 1.2 Å, is subtracted, the net width of the channels is 5.12 Å for F1, 4.87 Å for F2, and 4.80 Å for A, corresponding to the 4.7–5.3 Å range given for α-cyclodextrin.[19] Conversely, the average $O(3)_n\cdots O(2)_{n+1}$ hydrogen bond lengths show that the curvature of CA26 is clearly different from α-cyclodextrin and closer to β- or γ-cyclodextrin, depending on the enclosed guest molecules. This we associate with the cyclic structure of α-cyclodextrin contrasting the lock-washer structure of V-amylose with reduced curvature.

3. Discussion

Attempts to crystallize CA26-related CA containing 22–36 D-glucoses as such or as complexes with fatty acids and alcohols with 7–13 carbon atoms yielded only microcrystals in some cases that were not suitable for X-ray diffraction studies (except for those described here), suggesting that the size of the CA macrocycle and overhanging $–CH_2–CH_3$ termini are of importance for crystal packing and/or crystal growth. Structural differences between CA26 molecules in the fully hydrated CA26 and in complexes with polyiodide, undecanoic acid, and dodecanol are only minor if CA26 molecules are superimposed, indicating that the structure of CA26 remains virtually unchanged upon complex formation. In detail, however, structural differences associated with enclosed guest molecules may be important as shown in the present paper.

Hydrogen atoms C(3)–H, C(5)–H, and to a lesser extent C(6)–H that are located within the V-amylose channel contribute to H···H interactions with the aliphatic chains of undecanoic acid and dodecanol, but in different ratios for F1, F2, and A (Table 2). The modeling study of the complex formed by polymeric V-amylose and dodecanoic acid suggested that only the C(5)–H hydrogen atoms in the V-amylose channel determine the translational and rotational position of the fatty acid.[12] The here described complexes confirm this strong dependence on C(5)–H for F1 and A but not for F2 (where C(3)–H contributes equally well). Additionally, O(6) (in (+)-*gauche* orientation) and O(4) may be engaged in C–H···O hydrogen bonds with the guests, the $C(7F_1)$–H···$O(6)_{16}$ interaction causing even a bend ($C(6F_1)$–$C(7F_1)$–$C(8F_1)$–$C(9F_1)$, 135°) in the all-*trans* chain of undecanoic acid F1 (Fig. 4).

The bend in F2 ($C(3F_2)$–$C(4F_2)$–$C(5F_2)$–$C(6F_2)$, 130°) has no such clear correlation and must be attributed to differences in H···H and C–H···O interactions (see Table 2 and Fig. 5a and b). In the V-channel, F2 forms

many interactions to C(3)–H that provide more space so that the aliphatic chain is tilted with respect to the axis of the V-helix. This is associated with differences in the widths of the V-channels because the V-channel accommodating F2 is 0.21 Å narrower than that of F1 (Table 3) and might be too narrow to permit more H···H interactions with C(5)–H so that C(3)–H is accepted as interaction partner.

Crystal packing forces are expected to modulate the structure of CA26 in space groups $C2$ and $P2_12_12_1$. However, one could also invoke cooperative effects that do not occur for complex formation with dodecanol as it fits into the V-channels without significant structural distortions. By contrast, F1 and F2 feature strong, multi-contact binding of carboxyl groups to the O(6) end of the V-channels, and the CH_3 terminus of F2 (but not of F1) binds to the O(2), O(3) end through C–H···O interactions. This could be associated with structural changes of CA26 induced by binding of the first undecanoic acid molecule that destroys the C_2 symmetry of CA26, and the second undecanoic acid molecule has to accommodate in the structurally altered V-channel, leading to the differences observed for F1 and F2. A cooperative effect has actually been shown by isothermal titration calorimetry for inclusion of triiodide into CA26.[21]

Aliphatic chains in all-*trans* conformation and alcohols with slim head groups that are less demanding for hydrogen bonding than –COOH groups will fit smoothly into V-channels. Since the van der Waals diameter of the carboxyl group is ~5 Å, it would fit spatially into the V-channel provided that comparable hydrogen bonding interactions (with O(6) in (+)-*gauche* orientation) as with the O(6) end of the V-channels in CA26 may also be formed with polymeric V-amylose. This, however, would disrupt the regular V-helix that prefers the O(6) groups to be at (−)-*gauche*.[12,13] This agrees with the dodecanoic acid/V-amylose modeling study which found it unlikely that a fatty acid would enter the smooth V-helix.[12]

4. Conclusions

In the thus far known structures of CA26, the four C(6)–O(6) groups of D-glucoses G(1), G(7), G(14), and G(20) are systematically (+)-*gauche*. These O(6) groups and $O(6)_9$, $O(6)_{22}$ ((+)-*gauche*) form the binding sites for the carboxyl groups in **CA26·F** whereas in **CA26·A** only one hydrogen bond $O(1a)\cdots O(6)_{20}$ is formed. These hydrogen bonds must be considered special for CA26 as they are associated with the band-flips that do not occur in polymeric V-amylose. It is known, however, that inclusion complexes of V-amylose crystallize in plate-like, flaky forms in which the polymer chain is folded back and forth,[22] and there have been earlier suggestions that V-amylose in solution does not form a smooth helix but rather consists of short helical segments that are connected by unstructured (random) folds.[23,24] Since the folds are probably not fully unstructured and, as proposed previously,[13] at least partially associated with band-flips, they could also form in aqueous solutions of amylose, thereby providing binding sites for the carboxyl groups of fatty acids similar as in the here described complex with CA26.

This view is consistent with a solid state ^{13}C NMR investigation of V-amylose in complexes with a variety of long-chain fatty acids, some glycerol–fatty acid esters, and lysophosphatidylcholine in dry and hydrated states.[9] The aliphatic CH_2 groups inside the V-helical segments have the same chemical shifts, while the bulky carboxyl and glycerol head groups are mobile in the hydrated state and must, consequently, lie outside the V-channels. By contrast, aliphatic molecules with small head groups that are spatially less demanding than –COOH groups will fit smoothly into V-channels.

5. Experimental

CA26 was prepared and purified as described;[13] undecanoic acid and dodecanol were from SIGMA, Germany. A solution of CA26 in water (20 mg/mL) was mixed with 1.2-fold excess of undecanoic acid and sonicated at 50 °C for several minutes. Using the hanging drop vapor diffusion method, 3 μL of this solution and 3 μL of 25% (vol/vol) polyethyleneglycol (PEG) 400 (Merck) in water were equilibrated at 18 °C against a 10 mL reservoir containing 30% (vol/vol) PEG 400 in water. After several days, colorless needles of **CA26·F** grew, $0.6\times0.1\times0.1\,mm^3$. For **CA26·A**, corresponding procedures (without sonication) yielded plate-like crystals of dimensions $0.5\times0.3\times0.2\,mm^3$. One crystal each was sealed with a drop of mother liquor in a quartz capillary and used for X-ray diffraction data collection at 4 °C. For **CA26·F** crystals, X-ray data measured at $\lambda = 0.82$ Å (EMBL Outstation/DESY, Hamburg) using a Mar Research image plate detector were processed with the HKL package[25] to a resolution of 0.95 Å, and symmetry-equivalent data were merged. Data for **CA26·A** were collected with a Bruker CCD detector at $\lambda = 0.71073$ Å (MoK_α) at 1.0 Å resolution. The data were processed with Saint (Bruker) (Table 1).

The **CA26·A** crystal structure was determined by real/reciprocal space recycling procedure with SHELXD.[14] Starting with random atom distribution, the best solution was characterized by a correlation coefficient[26] of 0.86 and contained 140 correctly positioned atoms of the half CA26 molecule present in the asymmetric unit. The crystal structure of **CA26·F** was determined by molecular replacement with the program AmoRe[27] using CA26*ta* as search structure. After several cycles of full-matrix least-squares refinement with SHELX-97 in which

the glucose interatomic distances 1–2 and 1–3 were restrained,[28,29] water oxygen atoms were located from difference electron density maps using XtalView.[30] All atoms of CA26 were located (some O(6) hydroxyls disordered (+)- and (−)-*gauche*) and all atoms of the guest molecules except for the CH_2–CH_3 terminus of dodecanol that was not seen in the electron density. C–H hydrogen atoms were added in calculated positions at 0.97 Å (provided in SHELXL[14]), and temperature factors were refined anisotropically.[14] From final electron density maps, several (but not all) O–H hydrogen atoms of CA26 and of some water molecules could be located but since they were uncertain to some extent, they were not included in the refinement. For refinement statistics (see Table 1). Atomic coordinates, bond lengths, and bond angles have been deposited with the Cambridge Crystallographic Data Center under code CCDC 197411 for **CA26·F** and CCDC 197410 for **CA26·A**. They may be obtained on request from CCDC, 12 Union Road, Cambridge CB2 1EZ, UK (fax: +44-1223-336033; e-mail: deposit@ccdc.cam.ac.uk or http://www.ccdc.cam.ac.uk).

Acknowledgements

We thank Dr. Takeshi Takaha (Ezaki Glico Co. Ltd, Osaka, Japan) for providing purified samples of CA26 and Dr. W.-D. Hunnius (FU Berlin) for Raman measurements and discussions. We are grateful to Deutsche Forschungsgemeinschaft (Sa 196/29-3) and Fonds der Chemischen Industrie for financial support of this work and we thank EMBL/DESY Hamburg for synchrotron beamtime.

References

1. Morrison, W. R. In *Seed Storage Compounds: Biosynthesis, Interactions and Manipulation*; Shewry, P. R., Stobart, K., Eds.; Oxford University Press, 1993; pp 175–190.
2. Morrison, W. R.; Tester, R. F.; Snape, C. E.; Law, R.; Gidley, M. J. *Cereal Chem.* **1993**, *70*, 385–391.
3. Mercier, C.; Charbonniere, N.; Grebaut, J.; De la Gueriviere, J. F. *Cereal Chem.* **1980**, *57*, 4–9.
4. Krog, N. *Stärke* **1971**, *22*, 206–210.
5. Raphaelides, S.; Karkalas, J. *Carbohydr. Res.* **1988**, *172*, 65–69.
6. Sarko, A.; Zugenmaier, P. In *Fiber Diffraction Methods*; French, A. D., Gardner, K. C. H., Eds.; *ACS Symposium Series 141*; American Chemical Society: Washington, DC, 1980; pp 459–482.
7. Rappenecker, G.; Zugenmaier, P. *Carbohydr. Res.* **1981**, *89*, 11–19.
8. Godet, M. C.; Bizot, H.; Buléon, A. *Carbohydr. Polym.* **1995**, *27*, 47–52.
9. Snape, C. E.; Morrison, W. R.; Maroto-Valer, M. M.; Karkalas, J.; Pethrick, A. *Carbohydr. Polym.* **1998**, *36*, 225–237.
10. Karkalas, J.; Ma, S.; Morrison, W. R.; Pethrick, R. A. *Carbohydr. Res.* **1995**, *268*, 233–247.
11. Kowablansky, M. *Macromolecules* **1985**, *18*, 1776–1779.
12. Godet, M. C.; Tran, V.; Delage, M. M.; Buléon, A. *Int. J. Biol. Macromol.* **1993**, *15*, 11–16.
13. Gessler, K.; Usón, I.; Takaha, T.; Krauss, N.; Smith, S. M.; Okada, S.; Sheldrick, G. M.; Saenger, W. *Proc. Natl. Acad. Sci. U.S.A.* **1999**, *96*, 4246–4251.
14. Sheldrick, G. M.; Schneider, T. R. *Methods Enzymol.* **1997**, *277*, 319–343.
15. Nimz, O.; Gessler, K.; Usón, I.; Saenger, W. *Carbohydr. Res.* **2001**, *336*, 141–153.
16. Nimz, O.; Geßler, K.; Usón, I.; Laettig, S.; Welfle, H.; Sheldrick, G. M.; Saenger, W. *Carbohydr. Res.* **2003**, *338*, 977–986.
17. Jacob, J.; Gessler, K.; Hoffmann, D.; Sanbe, H.; Koizumi, K.; Smith, S. M.; Takaha, T.; Saenger, W. *Angew. Chem., Int. Ed. Engl.* **1998**, *37*, 606–609.
18. Jacob, J.; Gessler, K.; Hoffmann, D.; Sanbe, H.; Koizumi, K.; Smith, S. M.; Takaha, T.; Saenger, W. *Carbohydr. Res.* **1999**, *322*, 228–246.
19. Saenger, W.; Jacob, J.; Gessler, K.; Steiner, Th.; Hoffmann, D.; Sanbe, H.; Koizumi, K.; Smith, S. M.; Takaha, T. *Chem. Rev.* **1998**, *98*, 1787–1802.
20. Harata, K. In *Inclusion Compounds*; Atwood, J. L., Davies, J. E. D., MacNicol, D. D., Eds.; *Inorganic and Physical Aspects of Inclusion*; Oxford University Press: New York, 1991; Vol. 5, pp 311–344.
21. Kitamura, S.; Nakatani, K.; Takaha, T.; Okada, S. *Macromol. Rapid Commun.* **1999**, *20*, 612–615.
22. Helbert, W.; Chancy, H. *Int. J. Biol. Macromol.* **1994**, *16*, 207–213.
23. Hollo, J.; Szejtli, J. *Period. Polytech.* **1958**, *2*, 25–37.
24. Hollo, J.; Szejtli, J. *Brauwissenschaft* **1960**, *13*, 380–386.
25. Otwinowski, Z.; Minor, W. *Methods Enzymol.* **1996**, *276*, 307–326.
26. Fujinaga, M.; Read, R. J. *J. Appl. Cryst.* **1987**, *20*, 517–521.
27. Navaza, J. *Acta Cryst. A* **1994**, *50*, 157–163.
28. Sheldrick, G. M. In *Direct Methods for Solving Macromolecular Sructures*; Fortier, S., Ed.; Kluwer: Dordrecht, The Netherlands, 1998; pp 401–441.
29. Usón, I.; Sheldrick, G. M. *Curr. Opin. Struct. Biol.* **1999**, *9*, 643–648.
30. McRee, D. E. *Practical Protein Crystallography*; Academic: San Diego, 1993.
31. Kraulis, P. J. *J. Appl. Cryst.* **1991**, *24*, 946–950.
32. Merritt, E. A.; Bacon, D. J. *Methods Enzymol.* **1997**, *277*, 505–524.